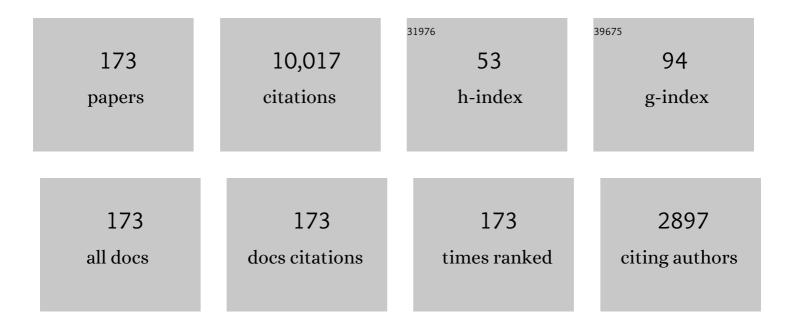
Thomas Eich

List of Publications by Year in descending order

Source: https://exaly.com/author-pdf/8648592/publications.pdf Version: 2024-02-01



THOMAS FICH

#	Article	IF	CITATIONS
1	Progress from ASDEX Upgrade experiments in preparing the physics basis of ITER operation and DEMO scenario development. Nuclear Fusion, 2022, 62, 042006.	3.5	15
2	I-mode pedestal relaxation events in the Alcator C-Mod and ASDEX Upgrade tokamaks. Nuclear Fusion, 2022, 62, 036004.	3.5	7
3	High-heat flux ball-pen probe head in ASDEX-Upgrade. Review of Scientific Instruments, 2022, 93, 023507.	1.3	5
4	Full- <i>f</i> electromagnetic gyrokinetic turbulence simulations of the edge and scrape-off layer of ASDEX Upgrade with GENE-X. Physics of Plasmas, 2022, 29, .	1.9	11
5	Edge transport and fuelling studies via gas puff modulation in ASDEX Upgrade L-mode plasmas. Nuclear Fusion, 2022, 62, 066035.	3.5	7
6	First-Principles Density Limit Scaling in Tokamaks Based on Edge Turbulent Transport and Implications for ITER. Physical Review Letters, 2022, 128, 185003.	7.8	19
7	Broadening of the power fall-off length in a high density, high confinement H-mode regime in ASDEX Upgrade. Nuclear Materials and Energy, 2021, 26, 100890.	1.3	26
8	Type-I ELM power loads on the closed outer divertor targets in the HL-2A tokamak. Nuclear Fusion, 2021, 61, 066024.	3.5	9
9	Optimization of the computation of total and local radiated power at ASDEX Upgrade. Nuclear Fusion, 2021, 61, 066025.	3.5	19
10	The separatrix operational space of ASDEX Upgrade due to interchange-drift-Alfvén turbulence. Nuclear Fusion, 2021, 61, 086017.	3.5	30
11	Gyrofluid simulation of an I-mode pedestal relaxation event. Physics of Plasmas, 2021, 28, 102502.	1.9	4
12	Physical mechanism behind and access to the I-mode confinement regime in tokamaks. Nuclear Fusion, 2020, 60, 096011.	3.5	20
13	Empirical study of gradient lengths ratio η e in the near SOL region in ASDEX Upgrade tokamak. Plasma Physics and Controlled Fusion, 2020, 62, 025005.	2.1	2
14	Turbulence driven widening of the near-SOL power width in ASDEX Upgrade H-Mode discharges. Nuclear Fusion, 2020, 60, 056016.	3.5	62
15	Scrape-off layer (SOL) power width scaling and correlation between SOL and pedestal gradients across L, I and H-mode plasmas at ASDEX Upgrade. Plasma Physics and Controlled Fusion, 2020, 62, 045015.	2.1	29
16	Correlation between near scrape-off layer power fall-off length and confinement properties in JET operated with carbon and ITER-like wall. Plasma Physics and Controlled Fusion, 2020, 62, 085004.	2.1	5
17	I-mode pedestal relaxation events at ASDEX Upgrade. Nuclear Fusion, 2020, 60, 126028.	3.5	20
18	Role of electric currents for the SOL and divertor target heat fluxes in ASDEX Upgrade. Plasma Physics and Controlled Fusion, 2020, 62, 105014.	2.1	7

#	Article	IF	CITATIONS
19	Overview of physics studies on ASDEX Upgrade. Nuclear Fusion, 2019, 59, 112014.	3.5	38
20	Analytic 1D approximation of the divertor broadening S in the divertor region for conductive heat transport. Plasma Physics and Controlled Fusion, 2019, 61, 085016.	2.1	0
21	Physics research on the TCV tokamak facility: from conventional to alternative scenarios and beyond. Nuclear Fusion, 2019, 59, 112023.	3.5	43
22	Dependence on plasma shape and plasma fueling for small edge-localized mode regimes in TCV and ASDEX Upgrade. Nuclear Fusion, 2019, 59, 086020.	3.5	34
23	A wall-aligned grid generator for non-linear simulations of MHD instabilities in tokamak plasmas. Computer Physics Communications, 2019, 243, 41-50.	7.5	10
24	Neutral pressure and separatrix density related models for seed impurity divertor radiation in ASDEX Upgrade. Nuclear Materials and Energy, 2019, 18, 166-174.	1.3	26
25	Effect of magnetic perturbation fields on power decay length in EMC3-EIRENE simulations and comparison to experiment in ASDEX upgrade. Nuclear Materials and Energy, 2019, 19, 205-210.	1.3	2
26	Synthetic edge and scrape-off layer diagnostics—a bridge between experiments and theory. Nuclear Fusion, 2019, 59, 086059.	3.5	8
27	Stationarity of I-mode operation and I-mode divertor heat fluxes on the ASDEX Upgrade tokamak. Nuclear Materials and Energy, 2019, 18, 159-165.	1.3	23
28	Effect of magnetic perturbations for ELM control on divertor power loads, detachment and consequences of field penetration in ASDEX Upgrade. Plasma Physics and Controlled Fusion, 2019, 61, 014008.	2.1	8
29	Correlation of the tokamak H-mode density limit with ballooning stability at the separatrix. Nuclear Fusion, 2018, 58, 034001.	3.5	57
30	Insights into typeâ€l edge localized modes and edge localized mode control from JOREK nonâ€linear magnetoâ€hydrodynamic simulations. Contributions To Plasma Physics, 2018, 58, 518-528.	1.1	16
31	Integrated simulations of H-mode operation in ITER including core fuelling, divertor detachment and ELM control. Nuclear Fusion, 2018, 58, 056020.	3.5	26
32	Parameter dependences of the separatrix density in nitrogen seeded ASDEX Upgrade H-mode discharges. Plasma Physics and Controlled Fusion, 2018, 60, 045006.	2.1	31
33	Dependence of the L-Mode scrape-off layer power fall-off length on the upper triangularity in TCV. Plasma Physics and Controlled Fusion, 2018, 60, 045010.	2.1	23
34	Scrape-off layer power fall-off length from turbulence simulations of ASDEX Upgrade L-mode. Plasma Physics and Controlled Fusion, 2018, 60, 085018.	2.1	13
35	Relating the near SOL transport with plasma properties of the confined edge region in ASDEX Upgrade. Plasma Physics and Controlled Fusion, 2018, , .	2.1	7
36	Parameter dependences of small edge localized modes (ELMs). Nuclear Fusion, 2018, 58, 112001.	3.5	47

#	Article	IF	CITATIONS
37	Effect of plasma geometry on divertor heat flux spreading: MONALISA simulations and experimental results from TCV. Nuclear Materials and Energy, 2017, 12, 893-898.	1.3	5
38	Density dependence of SOL power width in ASDEX upgrade L-Mode. Nuclear Materials and Energy, 2017, 12, 216-220.	1.3	6
39	A study on the density shoulder formation in the SOL of H-mode plasmas. Nuclear Materials and Energy, 2017, 12, 1189-1193.	1.3	22
40	Fast piezoelectric valve offering controlled gas injection in magnetically confined fusion plasmas for diagnostic and fuelling purposes. Review of Scientific Instruments, 2017, 88, 033509.	1.3	24
41	The physics and technology basis entering European system code studies for DEMO. Nuclear Fusion, 2017, 57, 016011.	3.5	84
42	Power exhaust by SOL and pedestal radiation at ASDEX Upgrade and JET. Nuclear Materials and Energy, 2017, 12, 111-118.	1.3	92
43	Comparative H-mode density limit studies in JET and AUG. Nuclear Materials and Energy, 2017, 12, 100-110.	1.3	13
44	Overview of progress in European medium sized tokamaks towards an integrated plasma-edge/wall solution ^a . Nuclear Fusion, 2017, 57, 102014.	3.5	23
45	ELM divertor peak energy fluence scaling to ITER with data from JET, MAST and ASDEX upgrade. Nuclear Materials and Energy, 2017, 12, 84-90.	1.3	116
46	Study of near SOL decay lengths in ASDEX Upgrade under attached and detached divertor conditions. Plasma Physics and Controlled Fusion, 2017, 59, 105010.	2.1	18
47	2D heat flux in ASDEX Upgrade L-Mode with magnetic perturbation. Nuclear Materials and Energy, 2017, 12, 1020-1024.	1.3	13
48	Assessment of divertor heat load with and without external magnetic perturbation. Nuclear Fusion, 2017, 57, 066045.	3.5	12
49	Electron temperature and heat load measurements in the COMPASS divertor using the new system of probes. Nuclear Fusion, 2017, 57, 116017.	3.5	27
50	Dynamic power balance analysis in JET. Physica Scripta, 2017, T170, 014035.	2.5	2
51	Progress in extrapolating divertor heat fluxes towards large fusion devices. Physica Scripta, 2017, T170, 014071.	2.5	13
52	Overview of the TCV tokamak program: scientific progress and facility upgrades. Nuclear Fusion, 2017, 57, 102011.	3.5	52
53	Divertor heat load in ASDEX Upgrade L-mode in presence of external magnetic perturbation. Plasma Physics and Controlled Fusion, 2017, 59, 095006.	2.1	24
54	Plasma–wall interaction studies within the EUROfusion consortium: progress on plasma-facing components development and qualification. Nuclear Fusion, 2017, 57, 116041.	3.5	75

#	Article	IF	CITATIONS
55	Real-Time Infrared Thermography at ASDEX Upgrade. Fusion Science and Technology, 2016, 69, 580-585.	1.1	10
56	Investigation of scrape-off layer and divertor heat transport in ASDEX Upgrade L-mode. Plasma Physics and Controlled Fusion, 2016, 58, 055015.	2.1	47
57	Interpretation of radiative divertor studies with impurity seeding in type-I ELMy H-mode plasmas in JET-ILW using EDGE2D–EIRENE. Journal of Nuclear Materials, 2015, 463, 135-142.	2.7	24
58	Divertor load footprint of ELMs in pellet triggering and pacing experiments at JET. Journal of Nuclear Materials, 2015, 463, 714-717.	2.7	11
59	Study of near scrape-off layer (SOL) temperature and density gradient lengths with Thomson scattering. Plasma Physics and Controlled Fusion, 2015, 57, 125011.	2.1	49
60	Real time capable infrared thermography for ASDEX Upgrade. Review of Scientific Instruments, 2015, 86, 113502.	1.3	67
61	Effect of nitrogen seeding on the energy losses and on the time scales of the electron temperature and density collapse of type-I ELMs in JET with the ITER-like wall. Nuclear Fusion, 2015, 55, 023007.	3.5	16
62	The H-mode density limit in the full tungsten ASDEX Upgrade tokamak. Plasma Physics and Controlled Fusion, 2015, 57, 014038.	2.1	70
63	Effect of resonant magnetic perturbations on low collisionality discharges in MAST and a comparison with ASDEX Upgrade. Nuclear Fusion, 2015, 55, 043011.	3.5	85
64	Partial detachment of high power discharges in ASDEX Upgrade. Nuclear Fusion, 2015, 55, 053026.	3.5	163
65	Thermal analysis of an exposed tungsten edge in the JET divertor. Journal of Nuclear Materials, 2015, 463, 415-419.	2.7	14
66	Scaling of the divertor power spreading (S-factor) in open and closed divertor operation in JET and ASDEX Upgrade. Journal of Nuclear Materials, 2015, 463, 49-54.	2.7	30
67	Change of the scrape-off layer power width with the toroidal B-field direction in ASDEX upgrade. Plasma Physics and Controlled Fusion, 2015, 57, 075005.	2.1	40
68	Improved equilibrium reconstructions by advanced statistical weighting of the internal magnetic measurements. Review of Scientific Instruments, 2014, 85, 123507.	1.3	2
69	Application of AXUV diode detectors at ASDEX Upgrade. Review of Scientific Instruments, 2014, 85, 033503.	1.3	63
70	DEMO divertor limitations during and in between ELMs. Nuclear Fusion, 2014, 54, 114003.	3.5	107
71	Impact of nitrogen seeding on confinement and power load control of a high-triangularity JET ELMy H-mode plasma with a metal wall. Nuclear Fusion, 2013, 53, 113025.	3.5	118
72	Impact of the ITER-like wall on divertor detachment and on the density limit in the JET tokamak. Journal of Nuclear Materials, 2013, 438, S139-S147.	2.7	76

#	Article	IF	CITATIONS
73	Outer target heat fluxes and power decay length scaling in L-mode plasmas at JET and AUG. Journal of Nuclear Materials, 2013, 438, S426-S430.	2.7	53
74	Simulations of tungsten transport in the edge of JET ELMy H-mode plasmas. Journal of Nuclear Materials, 2013, 438, S1005-S1009.	2.7	13
75	Material deposition and migration processes with resonant magnetic perturbation fields at TEXTOR. Journal of Nuclear Materials, 2013, 438, S602-S606.	2.7	5
76	Modification of scrape-off layer transport and turbulence by non-axisymmetric magnetic perturbations in ASDEX Upgrade. Journal of Nuclear Materials, 2013, 438, S64-S71.	2.7	18
77	Overview of ASDEX Upgrade results. Nuclear Fusion, 2013, 53, 104003.	3.5	36
78	Empiricial scaling of inter-ELM power widths in ASDEX Upgrade and JET. Journal of Nuclear Materials, 2013, 438, S72-S77.	2.7	65
79	Target particle and heat loads in low-triangularity L-mode plasmas in JET with carbon and beryllium/tungsten walls. Journal of Nuclear Materials, 2013, 438, S175-S179.	2.7	16
80	Experimental sheath heat transmission factors in diverted plasmas in JET. Journal of Nuclear Materials, 2013, 438, S393-S396.	2.7	9
81	Power load studies in JET and ASDEX-Upgrade with full-W divertors. Plasma Physics and Controlled Fusion, 2013, 55, 124039.	2.1	51
82	Estimation of edge electron temperature profiles via forward modelling of the electron cyclotron radiation transport at ASDEX Upgrade. Plasma Physics and Controlled Fusion, 2013, 55, 025004.	2.1	62
83	Scaling of the tokamak near the scrape-off layer H-mode power width and implications for ITER. Nuclear Fusion, 2013, 53, 093031.	3.5	448
84	Intermittent transport across the scrape-off layer: latest results from ASDEX Upgrade. Nuclear Fusion, 2013, 53, 073047.	3.5	17
85	Impurity seeding for tokamak power exhaust: from present devices via ITER to DEMO. Plasma Physics and Controlled Fusion, 2013, 55, 124041.	2.1	303
86	Solitary magnetic perturbations at the ELM onset. Nuclear Fusion, 2012, 52, 114025.	3.5	17
87	Optimized tokamak power exhaust with double radiative feedback in ASDEX Upgrade. Nuclear Fusion, 2012, 52, 122003.	3.5	106
88	Strike point splitting in the heat and particle flux profiles compared with the edge magnetic topology in a nÂ=Â2 resonant magnetic perturbation field at JET. Nuclear Fusion, 2012, 52, 054009.	3.5	36
89	Upgrade of the infrared camera diagnostics for the JET ITER-like wall divertor. Review of Scientific Instruments, 2012, 83, 10D530.	1.3	52
90	Radiative type-III ELMy H-mode in all-tungsten ASDEX Upgrade. Nuclear Fusion, 2012, 52, 122002.	3.5	11

#	Article	IF	CITATIONS
91	First Observation of Edge Localized Modes Mitigation with Resonant and Nonresonant Magnetic Perturbations in ASDEX Upgrade. Physical Review Letters, 2011, 106, 225004.	7.8	428
92	Integrated modelling of a JET type-I ELMy H-mode pulse and predictions for ITER-like wall scenarios. Plasma Physics and Controlled Fusion, 2011, 53, 124039.	2.1	23
93	Multi-parameter scaling of divertor power load profiles in D, H and He plasmas on JET and implications for ITER. Nuclear Fusion, 2011, 51, 083028.	3.5	31
94	Data acquisition and real-time bolometer tomography using LabVIEW RT. Fusion Engineering and Design, 2011, 86, 1129-1132.	1.9	9
95	Disruption mitigation by massive gas injection in JET. Nuclear Fusion, 2011, 51, 123010.	3.5	148
96	Moderation of target loads using fuelling and impurity seeding on JET. Journal of Nuclear Materials, 2011, 415, S313-S317.	2.7	15
97	Radiation losses of type-I ELMs during impurity seeding experiments in the full tungsten ASDEX Upgrade. Journal of Nuclear Materials, 2011, 415, S852-S855.	2.7	9
98	Influence of cross-field drifts and chemical sputtering on simulations of divertor particle and heat loads in ohmic and L-mode plasmas in DIII-D, AUG, and JET using UEDGE. Journal of Nuclear Materials, 2011, 415, S530-S534.	2.7	21
99	Overview of experimental preparation for the ITER-Like Wall at JET. Journal of Nuclear Materials, 2011, 415, S936-S942.	2.7	29
100	Radiation loads onto plasma-facing components of JET during transient events – Experimental results and implications for ITER. Journal of Nuclear Materials, 2011, 415, S821-S827.	2.7	18
101	Strike-point splitting induced by external magnetic perturbations: Observations on JET and MAST and associated modelling. Journal of Nuclear Materials, 2011, 415, S914-S917.	2.7	48
102	Interpretation of divertor Langmuir probe measurements during the ELMs at JET. Journal of Nuclear Materials, 2011, 415, S860-S864.	2.7	44
103	Heat load measurements on the JET first wall during disruptions. Journal of Nuclear Materials, 2011, 415, S817-S820.	2.7	22
104	Type-I ELM power deposition profile width and temporal shape in JET. Journal of Nuclear Materials, 2011, 415, S856-S859.	2.7	90
105	Plasma surface interactions in impurity seeded plasmas. Journal of Nuclear Materials, 2011, 415, S19-S26.	2.7	116
106	Power and particle fluxes to plasma-facing components in mitigated-ELM H-mode discharges on JET. Journal of Nuclear Materials, 2011, 415, S894-S900.	2.7	16
107	Coupling between JET pedestal ne–Te and outer target plate recycling. Journal of Nuclear Materials, 2011, 415, S421-S424.	2.7	1
108	Type-I ELM filamentary substructure on the JET divertor target. Journal of Nuclear Materials, 2011, 415, S865-S868.	2.7	16

#	Article	IF	CITATIONS
109	Power handling of a segmented bulk W tile for JET under realistic plasma scenarios. Journal of Nuclear Materials, 2011, 415, S943-S947.	2.7	16
110	Inter-ELM Power Decay Length for JET and ASDEX Upgrade: Measurement and Comparison with Heuristic Drift-Based Model. Physical Review Letters, 2011, 107, 215001.	7.8	370
111	Power load characterization for type-I ELMy H-modes in JET. Nuclear Fusion, 2011, 51, 123001.	3.5	26
112	Overview of ASDEX Upgrade results. Nuclear Fusion, 2011, 51, 094012.	3.5	27
113	First measurements of edge localized mode ion energies in the ASDEX Upgrade far scrape-off layer. Plasma Physics and Controlled Fusion, 2011, 53, 065002.	2.1	13
114	Poloidal distribution of recycling sources and core plasma fueling in DIII-D, ASDEX-Upgrade and JET L-mode plasmas. Plasma Physics and Controlled Fusion, 2011, 53, 124017.	2.1	22
115	Comparison between dominant NB and dominant IC heated ELMy H-mode discharges in JET. Nuclear Fusion, 2011, 51, 103033.	3.5	15
116	Studies of edge localized mode mitigation with new active in-vessel saddle coils in ASDEX Upgrade. Plasma Physics and Controlled Fusion, 2011, 53, 124014.	2.1	71
117	2D ECE measurements of type-I edge localized modes at ASDEX Upgrade. Nuclear Fusion, 2011, 51, 103039.	3.5	33
118	Characterization of edge profiles and fluctuations in discharges with type-II and nitrogen-mitigated edge localized modes in ASDEX Upgrade. Plasma Physics and Controlled Fusion, 2011, 53, 085026.	2.1	39
119	Data acquisition and real-time signal processing of plasma diagnostics on ASDEX Upgrade using LabVIEW RT. Fusion Engineering and Design, 2010, 85, 303-307.	1.9	18
120	Optimization of a bolometer detector for ITER based on Pt absorber on SiN membrane. Review of Scientific Instruments, 2010, 81, 10E132.	1.3	21
121	Observation of Confined Current Ribbon in JET Plasmas. Physical Review Letters, 2010, 104, 185003.	7.8	37
122	Overview of ELM Control by Low n Magnetic Perturbations on JET. Plasma and Fusion Research, 2010, 5, S2018-S2018.	0.7	13
123	Overview of ASDEX Upgrade results. Nuclear Fusion, 2009, 49, 104009.	3.5	11
124	Compatibility of ITER scenarios with full tungsten wall in ASDEX Upgrade. Nuclear Fusion, 2009, 49, 115014.	3.5	68
125	Overview of the results on divertor heat loads in RMP controlled H-mode plasmas on DIII-D. Nuclear Fusion, 2009, 49, 095013.	3.5	136
126	Disruption studies in ASDEX Upgrade in view of ITER. Plasma Physics and Controlled Fusion, 2009, 51, 124056.	2.1	71

#	Article	IF	CITATIONS
127	On the asymmetries of ELM divertor power deposition in JET and ASDEX Upgrade. Journal of Nuclear Materials, 2009, 390-391, 760-763.	2.7	42
128	Real time magnetic field and flux measurements for tokamak control using a multi-core PCI Express system. Fusion Engineering and Design, 2009, 84, 825-828.	1.9	12
129	ELM resolved energy distribution studies in the JET MKII Gas-Box divertor using infra-red thermography. Plasma Physics and Controlled Fusion, 2007, 49, 573-604.	2.1	75
130	Edge localized modes: recent experimental findings and related issues. Plasma Physics and Controlled Fusion, 2007, 49, S43-S62.	2.1	74
131	ELM transport in the JET scrape-off layer. Nuclear Fusion, 2007, 47, 1437-1448.	3.5	84
132	Active control of type-I edge localized modes on JET. Plasma Physics and Controlled Fusion, 2007, 49, B581-B589.	2.1	54
133	Chapter 4: Power and particle control. Nuclear Fusion, 2007, 47, S203-S263.	3.5	891
134	Transient heat loads in current fusion experiments, extrapolation to ITER and consequences for its operation. Physica Scripta, 2007, T128, 222-228.	2.5	124
135	Plasma wall interaction and its implication in an all tungsten divertor tokamak. Plasma Physics and Controlled Fusion, 2007, 49, B59-B70.	2.1	110
136	Divertor power deposition and target current asymmetries during type-I ELMs in ASDEX Upgrade and JET. Journal of Nuclear Materials, 2007, 363-365, 989-993.	2.7	38
137	Survey of Type I ELM dynamics measurements. Plasma Physics and Controlled Fusion, 2006, 48, A149-A162.	2.1	43
138	Filament structures at the plasma edge on MAST. Plasma Physics and Controlled Fusion, 2006, 48, B433-B441.	2.1	143
139	Power deposition onto plasma facing components in poloidal divertor tokamaks during type-I ELMs and disruptions. Journal of Nuclear Materials, 2005, 337-339, 669-676.	2.7	76
140	Radiation distribution and energy balance during type-I ELMs in ASDEX Upgrade. Journal of Nuclear Materials, 2005, 337-339, 756-760.	2.7	22
141	Edge and divertor physics with reversed toroidal field in JET. Journal of Nuclear Materials, 2005, 337-339, 146-153.	2.7	96
142	Integrated exhaust scenarios with actively controlled ELMs. Nuclear Fusion, 2005, 45, 502-511.	3.5	46
143	Type-I ELM substructure on the divertor target plates in ASDEX Upgrade. Plasma Physics and Controlled Fusion, 2005, 47, 815-842.	2.1	112
144	The spatial structure of type-I ELMs at the mid-plane in ASDEX Upgrade and a comparison with data from MAST. Plasma Physics and Controlled Fusion, 2005, 47, 995-1013.	2.1	71

#	Article	IF	CITATIONS
145	Overview of ASDEX Upgrade results—development of integrated operating scenarios for ITER. Nuclear Fusion, 2005, 45, S98-S108.	3.5	28
146	Characterization of the H-mode edge barrier at ASDEX Upgrade. Nuclear Fusion, 2005, 45, 856-862.	3.5	55
147	Impurity-seeded ELMy H-modes in JET, with high density and reduced heat load. Nuclear Fusion, 2005, 45, 1404-1410.	3.5	40
148	Observation of the palm tree mode, a new MHD mode excited by type-I ELMs on JET. Nuclear Fusion, 2005, 45, 201-208.	3.5	16
149	EDGE2D modelling of edge profiles obtained in JET diagnostic optimized configuration. Plasma Physics and Controlled Fusion, 2004, 46, 431-446.	2.1	64
150	Power deposition outside the divertor in ASDEX Upgrade. Plasma Physics and Controlled Fusion, 2004, 46, 971-979.	2.1	66
151	ITER-relevant H-mode physics at ASDEX Upgrade. Plasma Physics and Controlled Fusion, 2004, 46, B511-B525.	2.1	24
152	ELM pace making and mitigation by pellet injection in ASDEX Upgrade. Nuclear Fusion, 2004, 44, 665-677.	3.5	200
153	Characterization of pedestal parameters and edge localized mode energy losses in the Joint European Torus and predictions for the International Thermonuclear Experimental Reactor. Physics of Plasmas, 2004, 11, 2668-2678.	1.9	104
154	Reduction of divertor heat load in JET ELMy H-modes using impurity seeding techniques. Nuclear Fusion, 2004, 44, 312-319.	3.5	91
155	Stationary and transient divertor heat flux profiles and extrapolation to ITER. Journal of Nuclear Materials, 2003, 313-316, 759-767.	2.7	71
156	Edge localized mode physics and operational aspects in tokamaks. Plasma Physics and Controlled Fusion, 2003, 45, A93-A113.	2.1	88
157	Characteristics of type I ELM energy and particle losses in existing devices and their extrapolation to ITER. Plasma Physics and Controlled Fusion, 2003, 45, 1549-1569.	2.1	487
158	Nonaxisymmetric Energy Deposition Pattern on ASDEX Upgrade Divertor Target Plates during Type-I Edge-Localized Modes. Physical Review Letters, 2003, 91, 195003.	7.8	153
159	Steady-state and transient power handling in JET. Nuclear Fusion, 2003, 43, 999-1005.	3.5	14
160	The ASDEX Upgrade divertor IIb—a closed divertor for strongly shaped plasmas. Nuclear Fusion, 2003, 43, 1191-1196.	3.5	17
161	ELM frequency control by continuous small pellet injection in ASDEX Upgrade. Nuclear Fusion, 2003, 43, 1110-1120.	3.5	125
162	Overview of ASDEX Upgrade results. Nuclear Fusion, 2003, 43, 1570-1582.	3.5	20

#	Article	IF	CITATIONS
163	High density, high performance high-confinement-mode plasmas in the Joint European Torus (JET). Physics of Plasmas, 2002, 9, 2103-2112.	1.9	12
164	Interpretation of recent power width measurements in JET MkIIGB ELMy H-modes. Plasma Physics and Controlled Fusion, 2002, 44, 761-793.	2.1	20
165	Seeding of impurities in JET H-mode discharges to mitigate the impact of ELMs. Plasma Physics and Controlled Fusion, 2002, 44, 1879-1891.	2.1	19
166	ELM mitigation by nitrogen seeding in the JET gas box divertor. Plasma Physics and Controlled Fusion, 2002, 44, 639-652.	2.1	46
167	Confinement properties of high density impurity seeded ELMy H-mode discharges at low and high triangularity on JET. Plasma Physics and Controlled Fusion, 2002, 44, 1845-1861.	2.1	47
168	Characteristics and scaling of energy and particle losses during Type I ELMs in JET H-modes. Plasma Physics and Controlled Fusion, 2002, 44, 1815-1844.	2.1	153
169	Topological properties of the edge ergodic layer in tokamak plasma. IEEE Transactions on Plasma Science, 2002, 30, 66-67.	1.3	2
170	Steady state advanced scenarios at ASDEX Upgrade. Plasma Physics and Controlled Fusion, 2002, 44, B69-B83.	2.1	108
171	Plasma rotation induced by the Dynamic Ergodic Divertor. Nuclear Fusion, 2001, 41, 503-511.	3.5	16
172	Two dimensional modelling approach to transport properties of the TEXTOR-DED laminar zone. Nuclear Fusion, 2000, 40, 1757-1772.	3.5	41
173	First modelling of the TEXTOR DED near field divertor. Nuclear Fusion, 1998, 38, 515-529.	3.5	46